Membrane-Insertion Fragments of Bcl-x_L, Bax, and Bid†

Ana J. García-Sáez,‡ Ismael Mingarro,‡ Enrique Pérez-Payá,§ and Jesús Salgado*,‡

Departament de Bioquímica i Biologia Molecular, Universitat de València, and Fundación Valenciana de Investigaciones Biomédicas−Consejo Superior de Investigaciones Científicas (FVIB−CSIC), València, Spain

Received November 14, 2003; Revised Manuscript Received June 17, 2004

ABSTRACT: Apoptosis regulators of the Bcl-2 family associate with intracellular membranes from mitochondria and the endoplasmic reticulum, where they perform their function. The activity of these proteins is related to the release of apoptogenic factors, sequestered in the mitochondria, to the cytoplasm, probably through the formation of ion and/or protein transport channels. Most of these proteins contain a C-terminal putative transmembrane (TM) fragment and a pair of hydrophobic α helices (α5−α6) similar to the membrane insertion fragments of the ion-channel domain of diphtheria toxin and colicins. Here, we report on the membrane-insertion properties of different segments from antiapoptotic Bcl-x_L and proapoptotic Bax and Bid, that correspond to defined α helices in the structure of their soluble forms. According to prediction methods, there are only two putative TM fragments in Bcl-x_L and Bax (the C-terminal α helix and α-helix 5) and one in activated tBid (α-helix 6). The rest of their sequence, including the second helix of the pore-forming domain, displays only weak hydrophobic peaks, which are below the prediction threshold. Subsequent analysis by glycosylation mapping of single α-helix segments in a model chimeric system confirms the above predictions and allows finding an extra TM fragment made of helix α1 of Bax. Surprisingly, the amphipathic helices α6 of Bcl-x_L and Bax and α7 of Bid do insert in membranes only as part of the α5−α6 (Bcl-x_L and Bax) or α6−α7 (Bid) hairpins but not when assayed individually. This behavior suggests a synergistic insertion and folding of the two helices of the hairpin that could be due to charge complementarity and additional stability provided by turn-inducing residues present at the interhelical region. Although these data come from chimeric systems, they show direct potentiality for acquiring a membrane inserted state. Thus, the above fragments should be considered for the definition of plausible models of the active, membrane-bound species of Bcl-2 proteins.

The large group of proteins named Bcl-2 family (pBcl2)[1] are regulators of the release of apoptogenic factors from the mitochondria (*1*). Members of this family can be divided in three types, depending on their function and on the presence of different Bcl-2 homology domains, known as BH1−BH4 (*1*, *2*). Type-I pBcl2s, like Bcl-2 and Bcl-x_L, contain all four BH domains and have an antiapoptotic function. Type-II, like Bax and Bak, promote apoptosis and present domains BH1, BH2, and BH3, while type-III, like Bid and Bad, have also a proapoptotic effect but contain only domain BH3. Multiple lines of evidence connect the function of these proteins to their subcellular localization and their association with membranes. Thus, antiapoptotic, type-I pBcl2s are tail-anchored at the cytoplasmic side of mitochondrial, nuclear, and endoplasmic reticulum membranes, as in the case of Bcl-2 (*3*, *4*, *5*), or specifically to the mitochondrial outer membrane (MOM), as in the case of Bcl-x_L (*6*). In contrast, typical proteins from the two proapoptotic types, like Bax and Bid, are normally found soluble in the cytoplasm but, at the onset of apoptotic stimuli, migrate to the MOM and promote the release of cytochrome *c* and other apoptogenic factors (*7*−*9*).

The molecular mechanism of apoptosis regulation by pBcl2s is largely unknown, although there are a few well-accepted ideas in most proposed models. First, the antagonistic effect between pro- and antiapoptotic members of the family is thought to be connected to their ability to interact with each other through the BH3 domain of types II and III and a hydrophobic docking cleft found at the surface of type-I pBcl2s (*10*, *11*). This interaction-based mechanism is viewed either as a way to sequester proapoptotic factors by membrane-anchored type-I pBcl2s (*12*) or a way to inactivate these latter antiapoptotic regulators by proapoptotic ones (*13*). Either case leads to a model of mutual neutralization, where the ratio of pro- versus antiapoptotic pBcl2s determines apoptosis induction (*10*, *14*). Second, activation of typical proapoptotic type-II pBcl2s, like Bax, is accompanied by a change in their subcellular localization and an extensive structural reorganization, which facilitates membrane targeting and insertion to the MOM (*9*, *15*−*18*). This latter process is promoted by activated type-III pBcl2s (*9*, *19*−*22*), which in the case of

† This work was supported by grants from SALVAT Inquifarma, the Spanish MCyT (SAF2001 2811, BMC2003-01532), and MEC (FPU grant, to A.J.G.S.).

* To whom correspondence should be addressed: Departament de Bioquímica i Biologia Molecular, Universitat de València, C/ Dr. Moliner 50, 46100, Burjassot (València), Spain. Telephone: +34963543016. Fax: +34963544635. E-mail: jesus.salgado@uv.es.

‡ Universitat de València.

§ Fundación Valenciana de Investigaciones Biomédicas−Consejo Superior de Investigaciones Científicas (FVIB−CSIC).

[1] Abbreviations: pBcl2, proteins of the Bcl-2 family; MOM, mitochondrial outer membrane; TM, transmembrane; tBid, active C-terminal part of Bid after caspase-8 cleavage; Lep, engineered model membrane protein derived from leader peptidase of *E. coli*; AP, glycosyltransferase acceptor peptide; ISP, inhibitor of the signal peptidase.

10.1021/bi036044c CCC: $27.50
Published on Web 07/31/2004

Bid involves processing by caspase 8 to produce a C-terminal active form (tBid) (*23*, *24*). Third, once in the mitochondrial membrane, the type-II pBcl2s form oligomers, which may function as transmembrane (TM) pores and allow exit of cytochrome *c* to the cytoplasm (*25*−*27*).

Together with these established ideas, there are important opened questions. The mechanism of activation, targeting, and insertion of type-II pBcl2s is unknown. Thus, there is controversy about the mitochondrial targeting signal of Bax, which has been reported to be both at the N- (*16*, *28*) and C-terminal (*17*, *29*) regions. Activated BH3-only proteins, like tBid, and the mitochondria-specific lipid cardiolipin seem to collaborate in the translocation process (*30*, *31*), but how this is achieved is still not known. Also, the existence of specific protein receptors at the mitochondrial membrane has been proposed but not yet demonstrated (*32*, *33*). When the fact that oligomeric type-II pBcl2s form pores in the MOM is admitted, it is not clear whether these pores are made only of pBcl2s (*25*, *34*−*37*) or a combination of them with other mitochondrial pores, like components of the permeability transition pore (PTP) complex (*38*−*41*). Additionally, Bax and Bak have been found recently at the ER membrane, where they control apoptosis initiation dependent on the activation of caspase 12 (*42*). This new apoptotic pathway appears to be connected with the regulation of intracellular calcium fluxes (*43*, *44*). With respect to the molecular mechanism of inhibition of apoptosis by type-I pBcl2s, it is also a matter of debate, and various schemes, apart from the already mentioned BH3-dependent heterodimerization, have been proposed. These include inhibition of mitochondrial pores through direct protein−protein interaction (*40*, *45*), countering the effect of Bax channels (*46*), and control of Ca^{2+} homeostasis at the level of the ER (*47*, *48*).

To answer these open questions, structural information about the pBcl2s in the membrane is needed. The structures of water-soluble forms of Bcl-x_L (*49*, *50*), Bcl-2 (*51*), Bax (*52*), and Bid (*53*, *54*) have been solved. Despite the opposing roles of these proteins, they all show a remarkably similar, predominantly α-helical structure. Moreover, this structure resembles that of the pore-forming domain of colicins and diphtheria toxin, where two central predominantly hydrophobic α helices, α5 and α6 of Bcl-2, Bcl-x_L, and Bax (α6 and α7 in the case of Bid), are surrounded by a group of amphipathic ones (*49*, *55*). By analogy with the colicins, for which the mechanism of action has been studied in more detail (*55*, *56*), it was immediately proposed that the two central α helices might be responsible of the formation of TM pores (*49*), and this idea was indeed supported by measurements of ion-channel activity in synthetic lipid membranes for Bcl-x_L, Bcl-2, Bax, and Bid (*34*−*36*, *57*). Subsequent data support pore formation as part of the regulatory mechanism of the pBcl2s. Thus, oligomeric pores made by Bax are able to conduct the exit of cytochrome *c* from large lipid vesicles (*31*, *58*). Additionally, the possible importance of pore formation in the regulation of apoptosis by the pBcl2s is taking a renewed interest with the rediscovery of connections between the regulation of apoptosis and ER Ca^{2+} homeostasis (*42*, *44*, *59*−*61*).

Despite the wealth of circumstantial evidence in favor of the TM channel hypothesis, it has not been possible to conciliate this idea with a unified model, valid for pro- and antiapoptotic functions. A number of studies based on site-directed and deletion mutants prove the implication of the α-helices 5 and 6 in the ion-channel activity, cytotoxicity, release of cytochrome *c*, and apoptosis induction/regulation of pro- and antiapoptotic proteins (*46*, *62*−*64*). However, the generally assumed colicin-like model implies TM-spanning insertion of both the α5 and α6 fragments, of which there is only indirect or incomplete evidence (*63*−*66*). This is especially important because the above segments contain a significant number of (potentially) charged residues, which should in principle impose restrictions to a membrane-inserted state (*63*). It is also unknown whether other fragments participate in the formation of the channel. Undoubtedly, a better knowledge of the interaction of pBcl2s with lipid bilayers is needed to define consistent models of the functional structures of these proteins.

In this paper, we have studied the membrane-insertion properties of different fragments from Bcl-x_L, Bax, and Bid. When the sequences of these proteins are analyzed, TM character of various degrees can be predicted for different hydrophobic segments, which correspond to defined α helices in the structure of their soluble forms. Among them, we find the first α helix of the proposed pore-forming hairpins of Bcl-x_L, Bax, and Bid, but not the second α helix of these domains, which appears to be too polar to be defined apriori as a TM fragment. However, a transcription/translation/insertion assay by glycosylation mapping in fusions of an engineered model membrane protein derived from leader peptidase of *Escherichia coli* (Lep) manifests the capacity of the complete helical hairpin to insert across biological membranes, while we also find insertion for other fragments of low hydrophobicity. This paper provides the first evidence that hydrophobic segments, other than the C-terminal tail of Bcl-x_L, from paradigmatic pBcl2 proteins, can indeed insert across the membrane. The information reported here is a step forward toward the definition of reliable molecular models for the active structures of regulators of apoptosis from the Bcl-2 family.

EXPERIMENTAL PROCEDURES

Prediction of TM Segments. The sequences of Bcl-x_L, Bax, and Bid were analyzed for possible TM segments with the help of TopPedII (*67*) and DAS (*68*). A search for possible signal peptidase cleavage sites was made with the help of SignalIP (*69*). These programs were used via the Internet through available servers[2] and using standard parameters.

Enzymes and Chemicals. Plasmid pGEM1, RiboMAX SP6 RNA polymerase system, and rabbit reticulocyte lysate were from Promega (Madison, WI). [^{35}S]Met was from Amersham BioSciences. The PCR purification and RNeasy RNA clean up kits were from Qiagen (Hilden, Germany). The PCR mutagenesis kit QuikChange was from Stratagene (La Jolla, CA). The oligonucleotides were from the Isogen Bioscience (Maarssen, The Netherlands).

Construction of Lep/pBcl2 Fusions. Lep/pBcl2 chimeras were constructed through replacement of the H2 TM fragment of Lep (amino acid residues 59−81) by fragments from Bcl-x_L, Bax, or Bid. The plasmids encoding Lep (*70*), and

[2] URL localization of prediction methods used for this study: TopPredII, http://bioweb.pasteur.fr/seqanal/interfaces/toppred.html; DAS, http://www.sbc.su.se/~miklos/DAS/maindas.html; SignalIP, http://www.cbs.dtu.dk/services/SignalP.

the Lep$^{\Delta H1}$ version of this protein (*71*) were obtained from G. von Heijne (Stockholm University). DNA sequences encoding human Bcl-x_L and mouse Bax were obtained from G. Nuñez (University of Michigan Medical School), and a construct of human Bid was provided by X. Wang (University of Texas Southwestern Medical Center). Selected hydrophobic fragments of these proteins were amplified by PCR using forward and backward primers containing appropriate restriction sites. The PCR products were purified, digested, and ligated to the corresponding Lep vectors digested with the same enzymes. All constructs were confirmed by DNA sequencing.

In Vitro Mutagenesis. For the Bcl-$x_L^{\alpha5\alpha6[EEE]}$ fragment, the nucleotide codons for residues ^{166}Ile-Ala-Ala^{168} (numbering from the full-length human Bcl-x_L) were changed to Glu codons. For the Bcl-$x_L^{\alpha5[C151W]}$ and Bcl-$x_L^{\alpha5\alpha6[EEE][C151W]}$ fragments, the codon corresponding to C151 was changed to a Trp codon. The QuikChange kit (Stratagene) was used according to the protocol of the manufacturer. Mutations were confirmed by DNA sequencing.

In Vitro Transcription and Translation in Reticulocyte Lysate. In vitro transcription of Lep constructs was done as previously reported (*72*, *73*). The reaction mixtures were incubated at 37 °C for 2 h. The mRNAs were purified using a Qiagen RNeasy clean up kit and verified on a 1% agarose gel.

In vitro translation of the synthesized mRNA was done in the presence of reticulocyte lysate, [^{35}S]Met, and dog pancreas microsomes as described previously (*72*, *73*). After translation, the samples were analyzed by 10% SDS−PAGE. Assays were repeated in the presence of either a glycosylation acceptor tripeptide Ac-Asn-Tyr-Thr-NH_2, AP, or a non-acceptor tripeptide Ac-Gln-Tyr-Thr-NH_2, NAP (33 μM in both cases) (*73*). For the Lep/Bcl-$x_L^{\alpha5}$, Lep/Bax$^{\alpha5}$, Lep/Bid$^{\alpha6}$, and Lep/Bcl-$x_L^{\alpha5\alpha6[EEE]}$ constructs, the inhibitor of the mammalian signal peptidase *N*-methoxysuccinyl-Ala-Ala-Pro-Val-chloromethyl ketone, ISP (2 mM), from Sigma Chemical (St. Louis, MO) was used in control-reaction mixtures (*74*).

Alkaline Wash, Urea Treatment, and Triton X114 Partitioning. Alkaline extractions were performed according to ref *75*, and urea treatments were performed according to ref *76*. Briefly, after translation, mixtures containing microsomes were added to 4 volumes of either 100 mM Na_2CO_3 (pH 11.5) or 4 M urea (in 35 mM Tris-HCl at pH 7.4 and 140 mM NaCl buffer). The Na_2CO_3 and urea samples were clarified by centrifugation at 3000*g* and 4 °C for 10 min, and membranes were collected by layering the supernatant onto a 50-μL sucrose cushion and centrifugation at 100000*g* for 20 min at 4 °C. Finally, the pellet and supernatant were analyzed by 10% (Na_2CO_3-treated samples) or 12% (urea-treated samples) SDS−PAGE.

The Triton-X114 partitioning experiments were performed according to ref *76*. A total of 15 μL of hydrated Triton-X114 were added to 145 μL of the translation reactions containing microsomes, and the mixtures were incubated for 30 min on ice. The incubated Triton-X114 samples were equilibrated at 37 °C for 10 min to allow development of aqueous and organic phases (*77*). These phases were then separated by centrifugation at 10000*g* at room temperature. Subsequently, the lower, detergent-rich fraction was washed two times by addition of 10 volumes of fresh detergent-free buffer, followed by vortexing, incubation on ice for 30 min, and phase separation as before. The proteins present in the aqueous and detergent-rich fractions were finally precipitated in acetone and analyzed by 12% SDS−PAGE.

RESULTS

Prediction of TM Fragments of Bcl-x_L, Bax, and Bid. Interaction of pBcl2s with lipid membranes most likely involves insertion of hydrophobic protein segments, apart from the already well-characterized C-terminal tail of Bcl-x_L and the analogous C-terminal segment from Bax. To localize all possible TM fragments, the sequences of Bcl-x_L, Bax, and Bid were analyzed by using two prediction methods based on different principles. TopPred (*67*, *78*) performs essentially a hydropathy plot and requires no statistical parametrization. DAS (*68*), on the other hand, is based on the comparison of the query sequence with a set of known, nonhomologous membrane proteins and relies on the principle that the amino acid composition of TM fragments is more conservative than their sequence itself. The results of the predictions made with these two methods for the three pBcl2s studied in this paper are shown in Figure 1. Using the standard cutoff values of TopPred and the Kyte and Doolittle hydrophobicity scale (*79*), this program predicts two *certain* TM segments in the case of Bcl-x_L (residues 136−156 and 212−232, Figure 1A), two *certain* TM segments in the case of Bax (residues 107−127 and 170−190, Figure 1B), and one *certain* (residues 145−165) and one *putative* (residues 10−30) TM segments in the case of Bid (Figure 1C). The qualifications as *certain* or *putative* correspond to the standard output of TopPred and depend on the default cutoff hydrophobicity values of the program (*67*) (see the Experimental Procedures and Figure 1). When predictions were made with DAS (parts D−F of Figure 1), most probable TM segments were found to include residues 140−150 and 216−229 for Bcl-x_L, residues 110−122 and 172−185 for Bax, and residues 16−25 and 148−157 for Bid, which basically coincide with the TopPred prediction. The DAS profile is better resolved and shows an additional peak with significant TM propensity for a segment centered around residue 170 in the case of Bcl-x_L. Additionally, there are five peaks with DAS score values below the lower cutoff, although they are probably still significant. These are centered around residue 12 for Bcl-x_L, residues 27 and 139 for Bax, and residues 106 and 174 for Bid.

Interestingly, all hydrophobic fragments mentioned above almost coincide with defined α helices in the structures of soluble forms of Bcl-x_L, Bax, and Bid (Figure 2). Thus, the hydrophobic C-terminal segment of Bax corresponds to α-helix 9 in the structure of this protein. Bcl-x_L has an analogous C-terminal fragment, which was absent in the modified form of this protein used for the structure determination (*49*). This C-terminal tail is considered to form a TM anchor that, together with flanking basic amino acids, direct specific association of Bcl-x_L to the MOM (*6*). The second probable TM segment of Bax and Bcl-x_L corresponds to the central hydrophobic α-helix 5, found in the structure of both proteins. Adjacent to it, α-helix 6 is much less hydrophobic, especially in the case of Bax, because of the abundance of charged residues, which gives these segments an amphypathic character. With respect to Bid, the first hydrophobic segment of this protein is the first α helix found

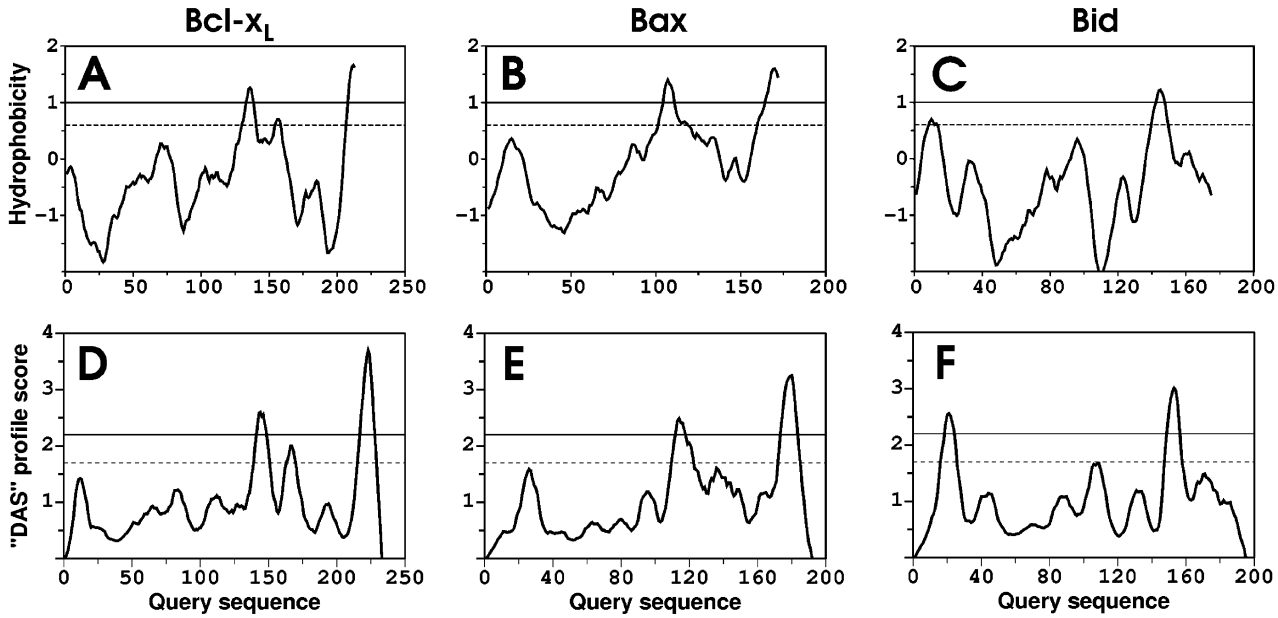

FIGURE 1: TM potency of the sequences of Bcl-x_L, Bax, and Bid as determined by prediction methods. (A) Bcl-x_L, (B) Bax, and (C) Bid are hydrophobicity plots made by using TopPred II (*67*) with default parameter settings. The horizontal lines indicate cutoff values for "certain" (—) and "putative" (- - -) TM fragments. (D) Bcl-x_L, (E) Bax, and (F) Bid are DAS (*68*) score profiles. Horizontal lines in this case correspond to score values of 2.0 (—) and 1.7 (- - -), which indicate high and low potential, respectively, in TM segments.

in its structure and the second corresponds to α-helix 6, which is analogous to α-helix 5 from Bcl-x_L and Bax. Each of these two segments belongs to a different fragment among the two formed after processing of Bid by caspase 8. Finally, we will consider four additional fragments that show low but probably significant DAS TM propensity. These roughly coincide with α-helix 1 from both Bcl-x_L and Bax and α-helices 4 and 7 from Bid.

Testing Membrane Insertion of pBcl2 Fragments: Membrane Insertion of Single Helix Bcl-x_L Fragments. Glycosylation mapping in a transcription/translation/insertion assay has been employed before to study insertion and topology of putative TM fragments in ER microsomal membranes (*80*). It consists on the use of a model, engineered TM protein derived from the leader peptidase of *E. coli* (Lep), with an N-terminal TM fragment (H1) followed by a highly positively charged loop (P1), a second TM segment (H2), and a soluble C-terminal domain (P2) with an engineered glycosylation acceptor site (Figure 3A). The flanking regions of the H1 fragment direct the insertion of the protein according to the "positive inside" rule (*81*), with the N terminus oriented toward the lumenal side of the microsomes. Thus, the protein will be glycosylated only when the fragment H2 inserts in the membrane, exposing the P2 glycosylation domain toward the lumen (Figure 3A). In such a system, the potential of a sequence to function as a TM segment can be tested by using it in place of the H2 fragment of Lep, in vitro transcribing and translating the corresponding chimera in the presence of ER microsomes, and finally checking for possible glycosylation through the observation of a ~2-kDa increase of expected molecular weight by SDS−PAGE (Figure 3B).

On the basis of the predictions made by TopPred and DAS, different peptide segments from Bcl-x_L, Bax, and Bid were selected for their analysis of membrane insertion using Lep chimeras (see Figures 1 and 2). The C-terminal hydrophobic segment of type-I Bcl2s has been previously shown to function as an anchoring tail that attaches this protein to the ER and outer mitochondrial membranes (*5*, *6*). As expected, when we assay the C-terminal putative TM segment from Bcl-x_L (Lep/Bcl-x_L^{Ct} construct) in the presence of ER microsomes, we observe the appearance of a new SDS−PAGE band corresponding to an increased molecular weight of the protein (lane 2 of Figure 4A). This band shift is due to glycosylation of Lep P2 at the lumenal side, because it attenuates with the use of a specific inhibitor of the microsomal glycosyltransferase (acceptor peptide, AP; lane 3 of Figure 4A), demonstrating TM insertion of the assayed Bcl-x_L^{Ct} sequence in the context of the Lep/Bcl-x_L^{Ct} chimera. Notably, modification of the fusion protein was not quantitative, which we attribute to incomplete or heterogeneous efficiency of the translocation/glycosylation machinery. No quantitative modifications are often observed in these types of experiments for putative TM fragments (*70*−*74*, *82*). We should also keep in mind that physiological membrane insertion of Bcl-2 proteins occurs post-translationally through a hitherto unknown mechanism independent of the ER translocon (*83*), which can be an additional reason for incomplete modification in this case. Nevertheless, because the TM character of this fragment offers no doubt (*5*, *6*), the results of Figure 4A can be considered as an internal positive control throughout this paper.

When a fusion containing the α-helix 5 from Bcl-x_L (Bcl-$x_L^{\alpha 5}$) was assayed, a band corresponding to a slightly lower molecular weight was obtained in the presence of microsomes (lane 2 of Figure 4B). This behavior suggest that digestion of the Lep/Bcl-$x_L^{\alpha 5}$ chimera is taking place. Treatment with AP allows the observation of an even lower molecular-weight band, demonstrating that the processed protein was also glycosylated (lane 3 of Figure 4B) and indicating that the domain P2 was translocated to the lumen of the microsomes through insertion of the Bcl-$x_L^{\alpha 5}$ segment across the membrane.

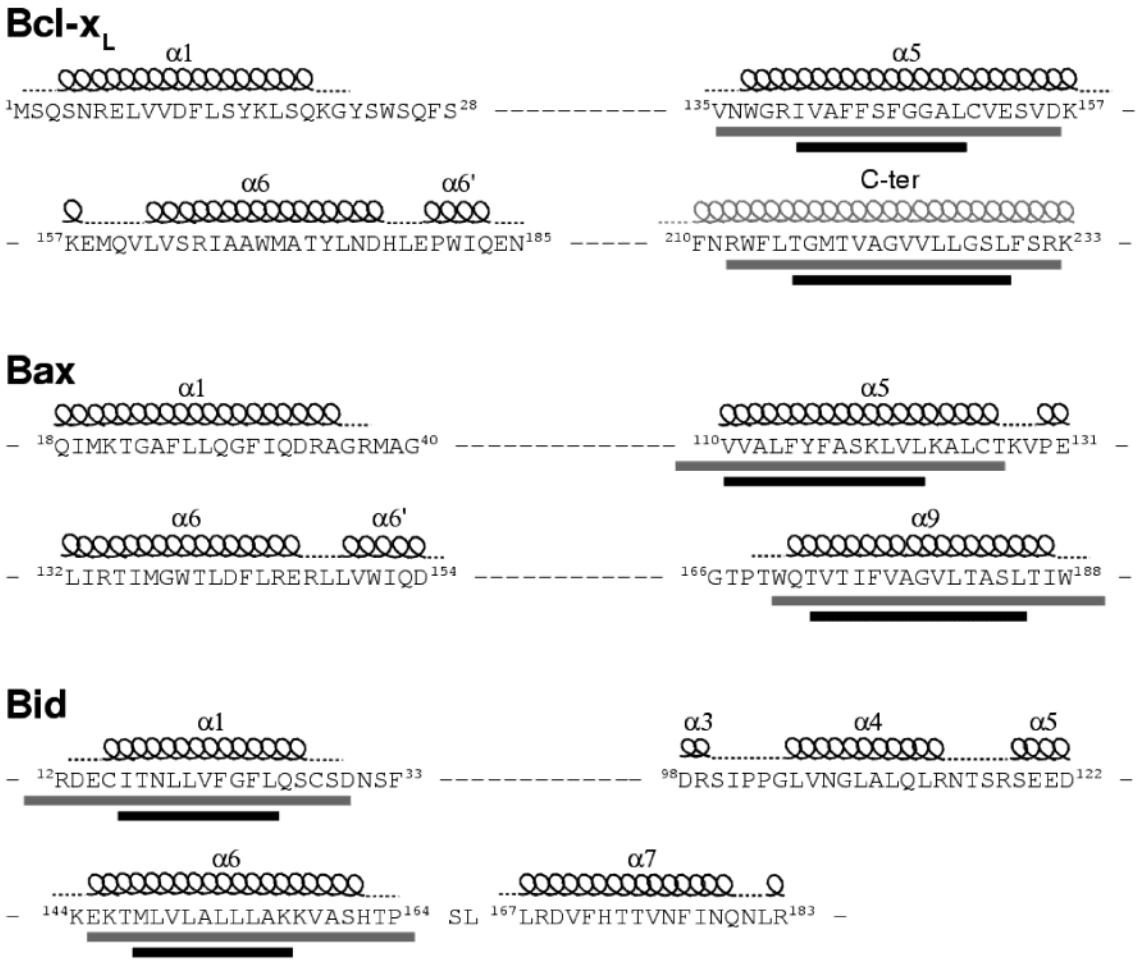

FIGURE 2: Schematic representation of the sequences of α helical segments from Bcl-x_L, Bax, and Bid. Only the segments studied in this paper are represented, with numbers in superscript indicating the first and last residue of assayed fragments (numbering corresponds to the full-length proteins). Positions of α helices are as reported for the structures of water-soluble forms of these proteins (*49*, *52*, *53*). In the case of the C-terminal tail of Bcl-x_L, the α-helix structure is hypothetical, because this fragment was deleted in the protein used for the structure determination (*49*). Possible TM segments, according to the TopPred II (*67*) and DAS (*68*) predictions, are indicated below the corresponding sequences as gray (TopPred II) and black (DAS) horizontal bars.

Observation of cleaved Lep chimeras in a similar assay has been previously reported, and it has been attributed to the activity of the microsomal signal peptidase (*74*, *82*). In agreement with this possibility, using an inhibitor of the mammalian signal peptidase (ISP) abolished digestion of Lep/Bcl-$x_L^{\alpha 5}$, and a faint band corresponding to full-length glycosylated Lep/Bcl-$x_L^{\alpha 5}$ is now observed (lanes 5 and 7 of Figure 4B). Interestingly, glycosylation is much more efficient after protein cleavage, because it has been observed before for a similar case (*82*). Although processing sites for signal peptidases usually contain low stringent sequences, SignalIP (*69*) allowed us finding a possible cleavage motif within the Bcl-$x_L^{\alpha 5}$ segment, consisting on the sequence ALC^{151}VE (numbering corresponding to full-length Bcl-x_L). Involvement of this motif in the processing of Lep/Bcl-$x_L^{\alpha 5}$ was tested by site-directed mutagenesis. As shown in Figure 4C, replacement of C151 by a tryptophane allows the observation of a normal-length glycosylation band, while processing is now almost completely impaired. All together, these data indicate that Bcl-$x_L^{\alpha 5}$ can act as a TM fragment, at least in the context of the Lep/Bcl-$x_L^{\alpha 5}$ chimera.

The sequences corresponding to the α-helices 1 and 6 from Bcl-x_L (Figure 2) were also tested for insertion in the Lep/Bcl-$x_L^{\alpha 1}$ and Lep/Bcl-$x_L^{\alpha 6}$ fusions. However, in these two latter cases, neither glycosylation nor cleavage was observed (parts D and E of Figure 4), indicating that none of the corresponding assayed fragments inserts across the microsomal membrane. This result is especially significant in the case of Bcl-$x_L^{\alpha 6}$, because according to the colicin-like model, it is part of the proposed membrane-insertion domain.

Testing TM Insertion of the α5−α6 Hairpin from Bcl-x_L. Although the absence of insertion for Bcl-$x_L^{\alpha 6}$ is in agreement with the predicted low-TM propensity (see Figure 1), it prompted us to question whether the surrounding protein context had an influence in the insertion tendency of this sequence. To test this possibility, a fragment corresponding to the α5−α6 hairpin (Bcl-$x_L^{\alpha 5\alpha 6}$) was assayed. As shown in Figure 4F, no glycosylation is observed for the Lep/Bcl-$x_L^{\alpha 5\alpha 6}$ chimera. This result is ambiguous, because both the simultaneous absence of insertion (Figure 4I) and the simultaneous insertion (Figure 4J) of the two helices of the hairpin can give rise to the observed pattern. The second possibility was challenged by assaying a mutant of Lep/Bcl-$x_L^{\alpha 5\alpha 6}$, where three hydrophobic residues from the center of α-helix 6 were replaced by glutamates (Lep/Bcl-$x_L^{\alpha 5\alpha 6[EEE]}$). Such a mutation should avoid insertion of α-helix 6, without affecting insertion of α-helix 5 (73). In this case, a pattern similar to the one obtained for Lep/Bcl-$x_L^{\alpha 5}$ is

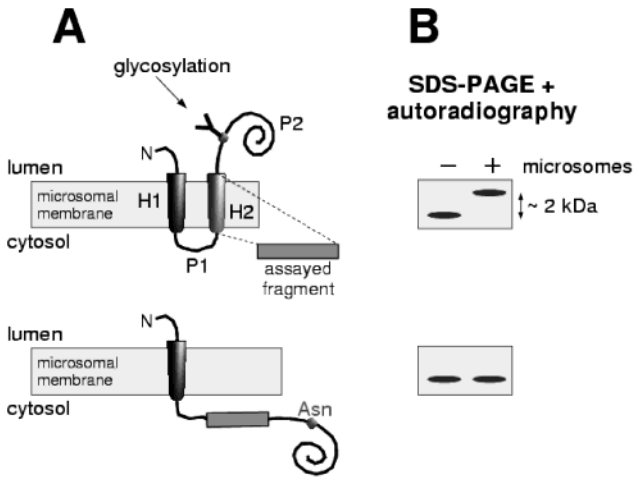

FIGURE 3: Topology of Lep and scheme of a glycosylation-mapping experiment. (A) TM fragment H1 inserts with the N terminus toward the lumen of microsomes. Assayed putative TM fragments are introduced in place of H2. Membrane insertion of the assayed H2 fragments places the domain P2 in the lumenal side, where it can be glycosylated at an engineered acceptor site (Asn90 residue). (B) Observation of a ~2-kDa band shift to a higher molecular weight means that P2 has been glycosylated and informs the membrane insertion of the H2 replacement fragment.

observed (Figure 4G), consisting of lower molecular-weight bands because of cleavage and glycosylation of the translocated C-terminal domain. Again, a C151W mutant of the latter construct (Figure 4H) proves that cleavage occurs at the ALC^{151}VE motive of α-helix 5, most likely by the microsomal signal peptidase, and the pattern represented in Figure 4K is observed. These data indicate that the absence of glycosylation in the case of the Lep/Bcl-$x_L^{\alpha5\alpha6}$ chimera was due to the simultaneous insertion of α-helices 5 and 6 (Figure 4J). Although with this topology, the ALC^{151}VE motive could be accessible for processing, the different protein context, with respect to the single-fragment construct or the Lep/Bcl-$x_L^{\alpha5\alpha6[EEE]}$ mutant, or structural restrictions imposed by a tight turn in the hairpin might render this case unfavorable for signal peptidase cleavage.

Additional support for the capacity of the Bcl-$x_L^{\alpha5\alpha6}$ hairpin to insert into microsomal membranes came from the use of a modified version of Lep, where the H1 TM fragment has been deleted and a second glycosylation site has been added in the P1 loop (Lep$^{\Delta H1}$, Figure 5A) (*71*). In this case, when H2 is replaced by a hairpin of two potential TM fragments, the insertion of only one of them can be clearly distinguished from the insertion of the two (parts B−D of Figure 5). The transcription of the Lep$^{\Delta H1}$/Bcl-$x_L^{\alpha5\alpha6}$ fusion gave no glycosylation (not shown), indicating that neither the P1 nor the P2 glycosylation sites were accessible at the inside of the microsomes. To rule out the possibility that the Lep$^{\Delta H1}$/Bcl-$x_L^{\alpha5\alpha6}$ fusion does not bind at all to the membranes, the microsomes were pelleted after a sodium carbonate wash. Under these conditions, the nonglycosylated protein was retained in the membrane fraction (lanes 1 and 2 of Figure 5E), suggesting that it binds tightly to the microsomal membranes through the Bcl-$x_L^{\alpha5\alpha6}$ hairpin.

Binding of Lep$^{\Delta H1}$/Bcl-$x_L^{\alpha5\alpha6}$ as an integral-membrane protein was further supported by treating the microsomes with urea and Triton-X114 (*76*, *77*). Incubation of the microsomal samples with 4 M urea, followed by ultracentrifugation, shows again that the protein appears mostly associated with the membrane fraction (lanes 1 and 4 of Figure 5F), as expected for an integral-membrane protein. The nonionic detergent Triton-X114 separates in aqueous and detergent-rich phases above the so-called "cloud point" temperature (20 °C) (*77*). It has been shown that membrane lipids and hydrophobic proteins partition to the detergent-rich phase, and this has been used to specifically isolate

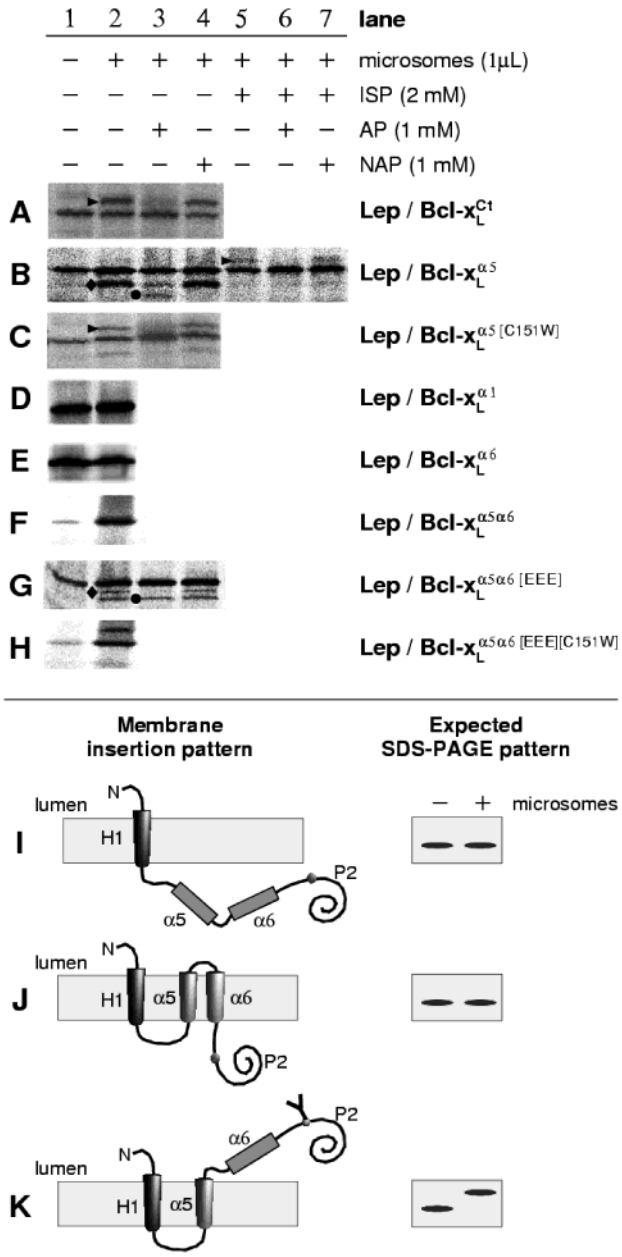

FIGURE 4: SDS−PAGE analysis of Lep/Bcl-x_L constructs. Fusions were expressed and labeled with [^{35}S]methionine in vitro in reticulocyte lysate in the absence (lane 1) and presence (lanes 2−7) of dog pancreas microsomes. Glycosylation gives rise to a higher molecular-weight band (marked with an arrowhead), which intensity is substantially reduced in the presence of an AP (lanes 3 and 6). A NAP is used as a control (lanes 4 and 7). In B and G, ◆ indicates a processed and glycosylated product and ● indicates a processed and nonglycosylated product. Processing is prevented in the presence of an inhibitor of the signal peptidase, ISP (lanes 5−7 of B) or by mutating residue C151 into a tryptophane (C and H). I−J represent possible membrane-insertion and expected SDS−PAGE patterns for the assays of wild-type and mutant double-helix Bcl-$x_L^{\alpha5\alpha6}$ fragments (shown in F−H).

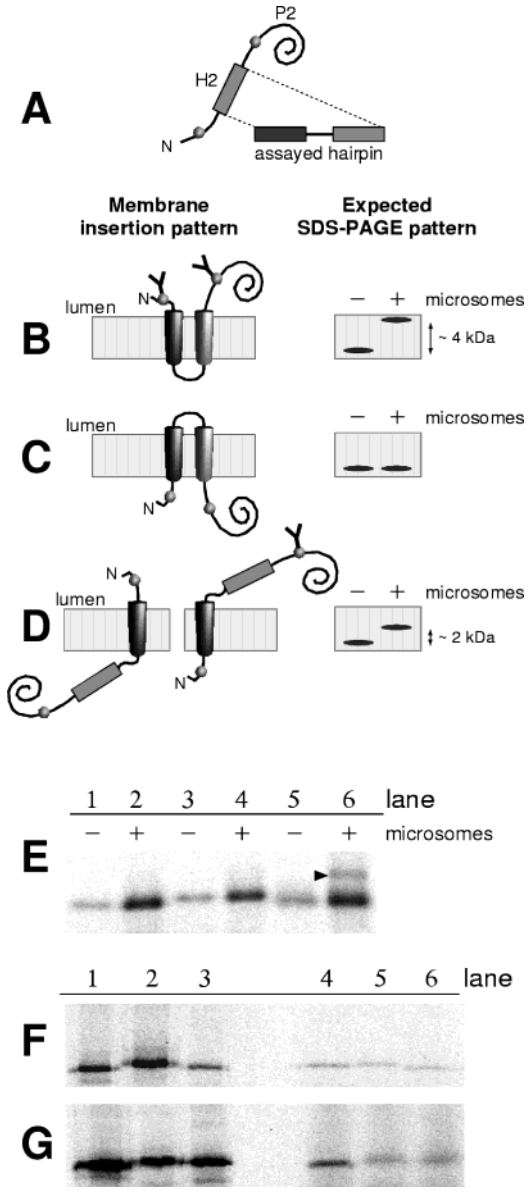

FIGURE 5: Schematic representation of possible membrane-insertion patterns and results of SDS−PAGE analysis of double-helix hairpins inserted in $Lep^{\Delta H1}$. (A) Two glycosylation sites are present in this construct, placed N and C terminal with respect to the assayed double helix. (B) Simultaneous insertion of both α helices should give rise to a doubly glycosylated product with a ~4-kDa molecular-weight increase or (C) to a normal-size nonglycosylated product. (D) Band shift corresponding to a ~2-kDa mass increase is due to the insertion of only one α-helical segment. E shows the results of in vitro expressions of [^{35}S]methionine-labeled $Lep^{\Delta H1}$/Bcl-$x_L^{\alpha5\alpha6}$ (lanes 1 and 2), $Lep^{\Delta H1}/Bax^{\alpha5\alpha6}$ (lanes 3 and 4), and $Lep^{\Delta H1}/Bid^{\alpha6\alpha7}$ (lanes 5 and 6) in reticulocyte lysate in the absence (lanes 1, 3, and 5) or presence (lanes 2, 4, and 6) of dog pancreas microsomes. All samples were alkaline-washed and pelleted before loaded in the gel. The band of glycosylated protein in lane 6 is marked with an arrowhead. In F, the pellet and supernatant after treatment of the microsomal samples with 4 M urea are shown for the $Lep^{\Delta H1}$/Bcl-$x_L^{\alpha5\alpha6}$ (lanes 1 and 4), $Lep^{\Delta H1}/Bax^{\alpha5\alpha6}$ (lanes 2 and 5), and $Lep^{\Delta H1}/Bid^{\alpha6\alpha7}$ (lanes 3 and 6). The SDS−PAGE analysis of hydrophobic (lanes 1−3) and aqueous (lanes 4−6) phases after Triton X114 treatment is shown in G, for $Lep^{\Delta H1}$/Bcl-$x_L^{\alpha5\alpha6}$ (lanes 1 and 4), $Lep^{\Delta H1}/Bax^{\alpha5\alpha6}$ (lanes 2 and 5), and $Lep^{\Delta H1}/Bid^{\alpha6\alpha7}$ (lanes 3 and 6).

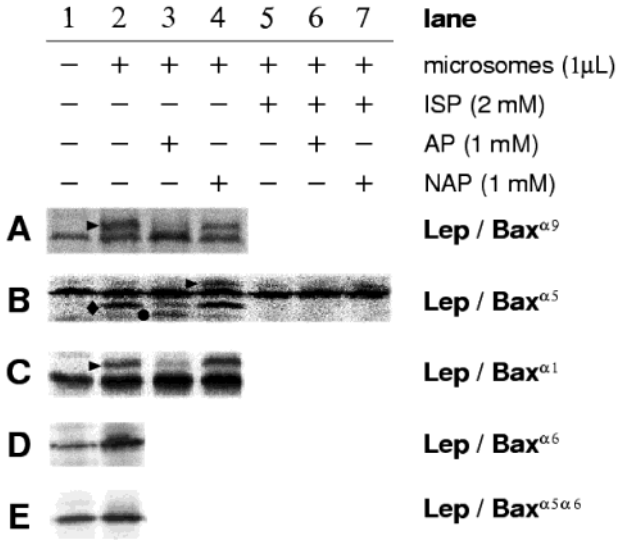

FIGURE 6: SDS−PAGE analysis of Lep/Bax constructs. In vitro translation products labeled with [^{35}S]methionine, in the absence (lane 1) and presence (lanes 2−7) of dog pancreas microsomes. For lanes 3 and 6, an AP was added in the reaction mixture, and for lanes 4 and 7, this was substituted by a NAP. Lanes 5−7 are from translation reactions containing an ISP. Marks indicate glycosylated products (arrowhead), processed and glycosylated products (◆), and processed and nonglycosylated products (●).

integral-membrane proteins (*76*, *77*, *84*). Preincubation of microsomal samples with 1% Triton-X114 at 0 °C, followed by incubation at 37 °C and centrifugation, allows detection of $Lep^{\Delta H1}$/Bcl-$x_L^{\alpha5\alpha6}$ mostly in the hydrophobic fraction (lanes 1 and 4 of Figure 5G). The latter three stringent treatments of the microsomes are consistent with tight binding of the chimera to the lipid membranes, as expected for TM insertion. Additionally, the absence of glycosylation of the membrane-associated protein means that insertion involves both helices of the α5−α6 hairpin.

Membrane Insertion of Bax Fragments. According to the predictions made above, the sequence of Bax contains various hydrophobic segments, which are analogous to similar fragments from Bcl-x_L (see Figure 1). Among them, the C-terminal tail corresponding to the α-helix 9 in the structure of soluble Bax ($Bax^{\alpha9}$) shows important hydrophobicity and DAS score peaks and is expected to function as a TM fragment. When the sequence of this fragment (Figure 2) replaces Lep H2, the Lep/$Bax^{\alpha9}$ fusion is glycosylated in the presence of microsomes (lanes 1−4 of Figure 6A), which agrees with membrane insertion of the assayed $Bax^{\alpha9}$ fragment. With respect to the hydrophobic α-helix 5 from Bax ($Bax^{\alpha5}$, Figure 2), it behaves as its analogous fragment from Bcl-x_L. Thus, the Lep/$Bax^{\alpha5}$ chimera gives a processed and glycosylated protein when translated in the presence of microsomes (Figure 6B), which indicates that $Bax^{\alpha5}$ can insert into the microsomal membrane. A possible cleavage site made of the sequence $ALC^{126}TK$ can also be found in the fragment $Bax^{\alpha5}$, and processing can be prevented in the presence of an inhibitor of the microsomal signal peptidase (Figure 6B). Additionally, as we have seen before, the full-length Lep/$Bax^{\alpha5}$ protein is barely glycosylated.

As a difference with respect to Bcl-x_L, the N-terminal α-helix 1 of Bax ($Bax^{\alpha1}$), which showed a modest hydrophobicity and DAS score (Figure 1), can adopt a TM position, as we deduce from the band of glycosylated protein that appeared when the Lep/$Bax^{\alpha1}$ chimera was assayed (Figure 6C).

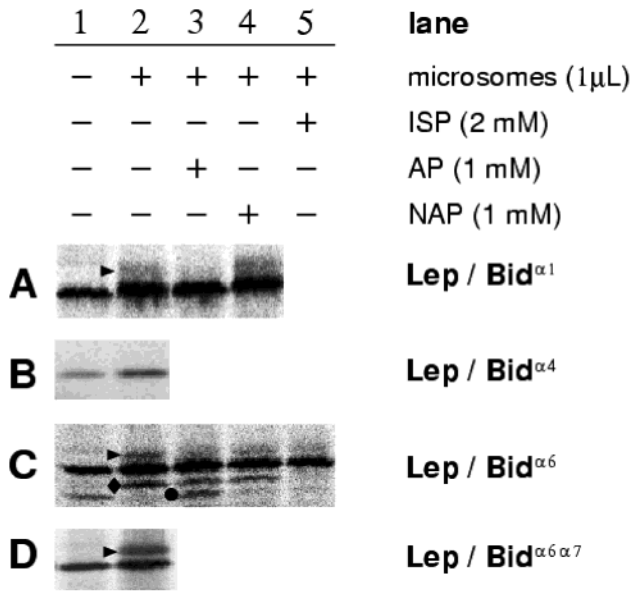

FIGURE 7: SDS−PAGE analysis of Lep/Bid constructs. Lep chimeras containing Bid hydrophobic fragments in place of TM domain H2 were translated in vitro using reticulocyte lysate and [^{35}S]methionine in the absence (lane 1) and presence (lanes 2−5) of dog pancreas microsomes. AP and NAP tripeptides were added in the reactions corresponding to lanes 3 and 4, respectively. Lane 5 is from translation reactions containing an ISP. Marks indicate glycosylated products (arrowhead), processed and glycosylated products (◆), and processed and nonglycosylated products (●).

With respect to α-helix 6 of Bax, when assayed alone in the corresponding Lep fusion (Lep/Bax$^{\alpha 6}$), it did not insert across the membrane, because no glycosylation was observed (Figure 6D).

Also in this case, we investigated the insertion behavior of the double-helix fragment Bax$^{\alpha 5\alpha 6}$. As shown in Figure 6E, the Lep/Bax$^{\alpha 5\alpha 6}$ chimera is neither glycosylated nor processed when translated in the presence of microsomes. Because, again, this result is ambiguous (see parts I and J of Figure 4), we prepared and analyzed a Lep$^{\Delta H1}$/Bax$^{\alpha 5\alpha 6}$ chimera. After translation in the presence of microsomes, the pellet of alkaline-washed membranes shows only the nonglycosylated Lep$^{\Delta H1}$/Bax$^{\alpha 5\alpha 6}$ protein (lanes 3 and 4 of Figure 5E). Similar to the case of Lep$^{\Delta H1}$/Bcl-x$_L^{\alpha 5\alpha 6}$ (see above), the urea and Triton-X114 treatments also agree with tight association of the Bax chimera with the membrane (lanes 2 and 5 of parts F and G of Figure 5), which supports the simultaneous insertion of the two helices of the Bax$^{\alpha 5\alpha 6}$ hairpin.

Membrane Insertion of Bid Fragments. The hydropathy profile of this BH3-only protein is clearly different from those of Bcl-x$_L$ and Bax (see Figure 1). Here, two possible TM segments can be found, made of α-helices 1 (Bid$^{\alpha 1}$) and 6 (Bid$^{\alpha 6}$) of the structure of the soluble protein (Figure 2), although only the second of them belongs to the active fragment tBid. Additionally, α-helix 4 (Bid$^{\alpha 4}$) also displays appreciable hydrophobicity (Figure 1).

When the Lep/Bid$^{\alpha 1}$ chimera is assayed, a faint higher molecular-weight band is observed in the presence of microsomes (Figure 7A). This is due to glycosylation of the protein, because it is not observed in the presence of AP and indicates a weak tendency of the Bid$^{\alpha 1}$ fragment to insert into the membrane. The weakly hydrophobic Bid$^{\alpha 4}$ fragment does not act as a TM (Figure 7B). With respect to the Bid$^{\alpha 6}$, assaying the corresponding Lep chimera resulted in a pattern similar to the one found for Bcl-x$_L^{\alpha 5}$ and Bax$^{\alpha 5}$ (see above), although the amount of full-length glycosylated chimera is somewhat higher. Thus, in this case, both lower and a higher molecular-weight bands were observed in the presence of microsomes (lane 2 of Figure 7C). Treatment with the AP inhibitor shows that the two new bands correspond to glycosylated proteins (lane 3 of Figure 7C). Additionally, treatment with the signal peptidase inhibitor shows that the lower molecular-weight band was a processed chimeric protein (lane 5 of Figure 7C). A possible cleavage site (VAS^{161}HT) was also found in the sequence of Bid$^{\alpha 6}$ with the help of SignalIP (*69*).

Finally, we assayed the hairpin α6−α7 from Bid, which despite the low hydrophobicity of the fragment α7 is also considered as a colicin-like insertion domain. A Lep fusion containing this sequence (Lep/Bid$^{\alpha 6\alpha 7}$) gave rise to a higher molecular-weight glycosylation band (Figure 7D), indicating insertion of only α-helix 6. Similar to the previous cases, the modification was not quantitative, which we attribute to incomplete efficiency of the translocation process. However, because here we are assaying a double-helix fragment, chances are that the pool of unmodified protein contains species where both helices were successfully inserted (see Figure 4J). To test this possibility, a chimera of the Lep$^{\Delta H1}$ model protein was assayed. The result is shown in lanes 5 and 6 of Figure 5E. Part of the protein appears as a band corresponding to glycosylation of one site, which is due to the TM insertion of just one fragment (Figure 5D), most likely the more hydrophobic α-helix 6. However, most of the Lep$^{\Delta H1}$/Bid$^{\alpha 6\alpha 7}$ fusion retained after alkaline wash is not glycosylated, corresponding to insertion of both α-helix 6 and 7. The urea and Triton-X114 treatments (lanes 3 and 6 of parts F and G of Figure 5) support that the Lep$^{\Delta H1}$/Bid$^{\alpha 6\alpha 7}$ chimera is an integral-membrane protein.

DISCUSSION

Although the association of pBcl2 proteins with intracellular lipid membranes is crucial for their function, little is known about the characteristics of this interaction. Activation of Bax is accompanied by translocation to the mitochondrial outer membrane, an extensive structural change, membrane insertion, and oligomerization (*9*, *16*, *17*, *26*). This is facilitated by tBid (*22*), which also translocates and inserts into the MOM (*9*, *85*). With respect to antiapoptotic Bcl-x$_L$, it constitutively resides at the MOM, anchored through a C-terminal tail (*6*). However, also in this latter case, a more extensive membrane insertion should be hypothesised to explain the ion-channel activity observed in vitro (*34*) and the heterodimerization-independent regulation of cell survival reported in vivo (*46*). Indeed, a change of membrane topology that implies insertion of α-helix 5 has been recently observed in the case of Bcl-2 as a consequence of apoptosis induction (*65*). One way to gain knowledge about the structures of the active, membrane-bound species of pBcl2s is by defining those segments that can be directly involved in membrane insertion.

Prediction of TM fragments of possible membrane proteins can be performed by using a number of different algorithms. In the absence of known membrane proteins, which are homologous to the query sequence, the choice is restricted

to methods that use single sequence information. In this study, we have used two of the such methods based on different principles. TopPred takes into account apriori principles, like hydrophobicity of the target sequence, and extra information in the form of the distribution of positively charged residues (the "positive inside" rule) (*78*). On the other hand, the analysis of DAS is of statistical nature, because it involves an indirect comparison of the query sequence with a collection of nonhomologous, known TM proteins (*68*). The good agreement that we find in the output of both methods is significant and suggests a possible TM character, of different degrees, for various segments of Bcl-x_L, Bax, and Bid, corresponding to defined α helices of their soluble structures (Figures 1 and 2). These predictions are tested through glycosylation-mapping experiments, revealing that some weakly hydrophobic segments (below the threshold of prediction) can also act as a TM fragment. Notably, among these latter fragments are those corresponding to the second α helix of the proposed pore-forming domains, which insert in the membrane only as part of a double-helix hairpin.

TM Insertion of C- and N-Terminal Helices. The C-terminal part of type-I and type-II pBcl2 proteins contain a canonical TM fragment. In the case of Bcl-x_L, this has been reported to form a TM-anchoring tail, where specific targetting to the MOM depends on the presence of, at least, two basic residues in the flanking ends (*6*). Here, we confirm the TM character of this sequence, because it is able to insert across the ER microsomal membrane in a Lep chimera.

The C-terminal region of Bax, that includes α-helix 9 and the upstream connecting loop, has been shown to be necessary and sufficient for this protein to target the MOM during apoptosis (*29*). The loop residue Pro168 controls the conformational change that is necessary to release the α-helix 9 from its firmly stabilized position in a hydrophobic cleft of the inactive soluble structure of the protein. We find that Bax$^{\alpha 9}$, including the residues of the preceding loop, can function as a TM-spanning fragment, at least, in a Lep chimera.

At the N-terminal part of the three pBcl2 proteins studied here, the most hydrophobic fragment corresponds to α-helix 1 of Bid (Figure 1), which does not belong to the active fragment, tBid, formed after caspase-8 cleavage. However, glycosylation mapping shows that TM propensity of Bid$^{\alpha 1}$ is very weak (Figure 7A). In agreement with this result, no membrane binding has been reported for the N-terminal piece of caspase-8-processed Bid. The function of the Bid$^{\alpha 1}$ hydrophobic fragment is most probably controlling the accessibility of the hydrophobic surfaces of the domain BH3 and the putative TM fragment Bid$^{\alpha 6}$ (*53*).

On the other hand, the main difference between the membrane-insertion analysis of Bax and Bcl-x_L is the behavior of the first α helix of these two proteins. From an NMR structural study of Bcl-x_L in detergent micelles, Bcl-$x_L^{\alpha 1}$ was proposed to be able to interact with lipid membranes (*86*). However, we found no evidence of membrane insertion from the analysis of the Lep/Bcl-$x_L^{\alpha 1}$ chimera. Conversely, fragment Bax$^{\alpha 1}$ is found to insert across the membrane. The reason for the different behavior of the Bcl-$x_L^{\alpha 1}$ and Bax$^{\alpha 1}$ fragments might be the larger number of charged residues and the shorter stretch of consecutive hydrophobic residues in the first one (see Figure 2).

The sequence of α-helix 1 from the structure of water-soluble Bax and the Bax$^{\alpha 1}$ fragment analyzed here (Figure 2) overlap with a proposed N-terminal mitochondrial-targetting region (residues 20−37) (*28*) Association of chimeric proteins containing this N-terminal segment with mitochondria was found to be alkaline-sensitive, suggesting that this sequence does not function as a TM domain but rather as a targeting sequence that interacts peripherally with the MOM (*28*). However, it starts to become clear (*18*) that the activation/membrane insertion of Bax is a multistep process, where both peripherally bound and membrane-inserted forms may be intermediate species (see below).

TM Bcl-$x_L^{\alpha 5\alpha 6}$, Bax$^{\alpha 5\alpha 6}$, and Bid$^{\alpha 6\alpha 7}$ Hairpins: Evidence of a Synergistic Insertion. Because of structural analogy with the ion-channel-forming domains of diphtheria toxin and bacterial colicins, the α5−α6 helical hairpin (α6−α7 of Bid) is regarded as a pore-forming domain. Site-directed mutagenesis and deletion studies support this idea and show that the α5−α6 hairpin of Bcl-x_L (or its homologous Bcl-2) is important for the ion-channel activity of this protein in vitro (*36*) and for its cytoprotective and antiapoptotic activities, independent of BH3 binding, in vivo (*46*, *62*). In the case of Bax, similar studies show the importance of this domain for mitochondrial localization and interaction with Bcl-x_L (*63*), as well as for the insertion to the mitochondrial membrane and the release of cytochrome *c* (*64*).

The colicin-like model involves TM insertion of the central α-helical hairpin, which apart from hydrophobic residues, also contains a significant number of acidic and basic residues (Figure 8). Here, we find that the firts helices of the hairpin, α5 from Bcl-x_L and Bax and its analogous α6 from Bid, can be predicted as clear TM fragments. However, if we were to consider sequence data alone, the accompanying α helix from the proposed pore-forming domain (α6 of Bcl-x_L and Bax and α7 of Bid) would only qualify as a potential TM (although mildly) in the case of Bcl-x_L (see Figure 1). The analysis of Lep chimeras shows that Bcl-$x_L^{\alpha 5}$, Bax$^{\alpha 5}$, and Bid$^{\alpha 6}$ can act as TM fragments. In these cases, glycosylation occurs together with processing by the microsomal signal peptidase. Nevertheless, this modification appears to be dependent on the protein context because it is not found in the case of the double-helix constructs (Figures 4D, 6E, and 7D). Thus, the observed cleavage is most likely a coincidence of no physiological significance, similar to that observed in other glycosylation-mapping experiments (*82*), that anyhow implies membrane insertion.

In agreement with membrane insertion of Bcl-$x_L^{\alpha 5}$, it has been recently reported that Cys158 of Bcl-2, that belongs to the α-helix 5 of this tail-anchored antiapoptotic protein, is protected from chemical modification upon induction of apoptosis and in response to BH3 peptides (*65*). These data strongly indicate that Bcl-2 is activated through a topology change that involves TM insertion of α5. Moreover, because the protein remains anchored through the C-terminal tail (*65*), the simultaneous insertion of α6 can also be implied. This is in line with a preliminary solid-state NMR investigation on Bcl-x_L, which suggests that α-helices 5 and 6 insert in the membrane (*66*).

In our study, evidence for insertion of the second helices of the hairpins, Bcl-$x_L^{\alpha 6}$, Bax$^{\alpha 6}$, and Bid$^{\alpha 7}$, was only found when the complete hairpins were assayed. Moreover, a rough comparison of the amounts of inserted protein in the Lep

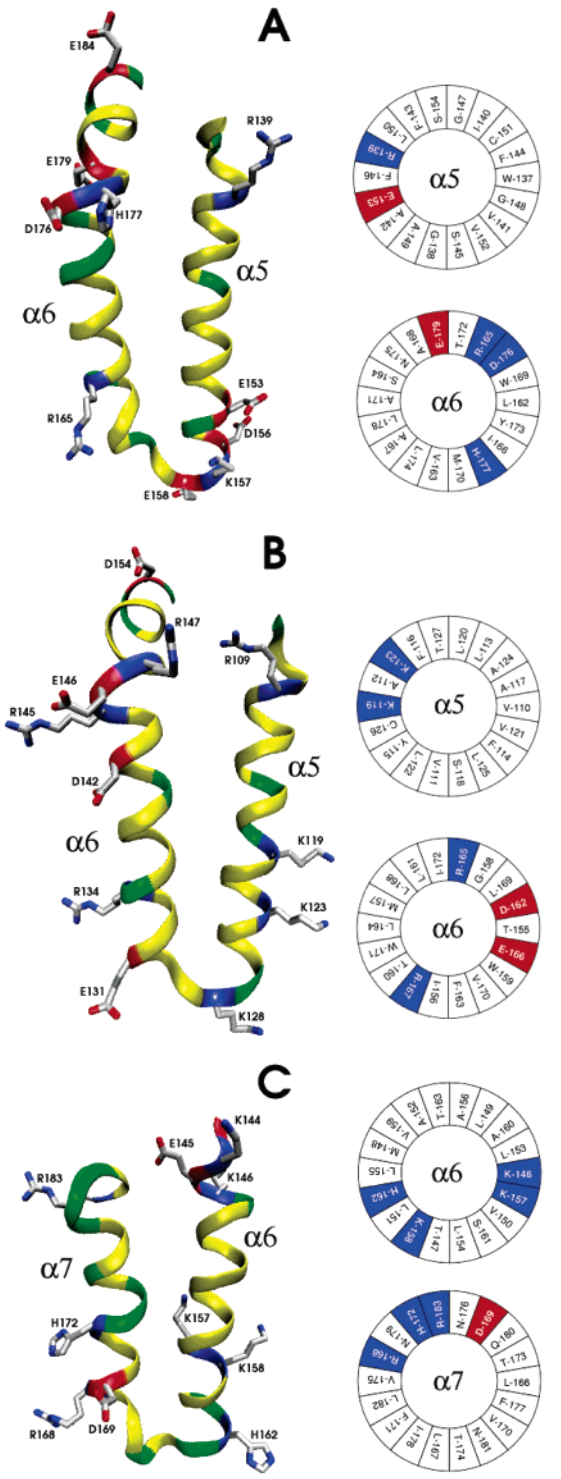

FIGURE 8: Ribbon structures and helix-wheel representations of α-helices 5 and 6 of Bcl-x_L (A) and Bax (B) and α-helices 6 and 7 of Bid (C). The hairpin structures are part of the determined 3D structures of soluble forms of human Bcl-x_L [PDB ID 1MAZ (*49*)], human Bax [PDB ID 1F16 (*52*)], and human Bid [PDB ID 2BID (*54*)]. The α5−α6 hairpin sequence of mouse Bax, used by us in this study, differs from that of human Bax by only Val^{150} to Gly replacement. The colors red, blue, green, and yellow in the ribbon figures correspond to acidic, basic, polar, and hydrophobic residues, respectively. The side chains of acidic and basic residues are represented as bonds, with colors red, blue, and gray used for oxygen, nitrogen, and carbon, respectively. For the helix wheels, only the 18 most central residues are represented. Potentially charged residues, both acidic and basic, are written with bold white characters over a red (acidic) or blue (basic) background. Residues are numbered according to the corresponding full-length proteins.

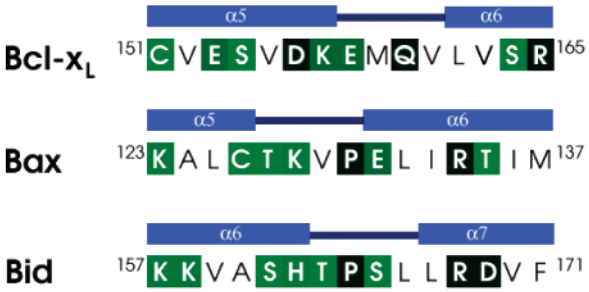

FIGURE 9: Turn-inducing propensity at the interhelical regions of hairpins Bcl-$x_L^{\alpha5\alpha6}$, $Bax^{\alpha5\alpha6}$, and $Bid^{\alpha6\alpha7}$, according to the scale of von Hejne and co-workers (*88*). Stretches of 15 residues are shown, with the numbers for the first and last residue as superscript (numbering corresponds to the full-length proteins). Residues written in plain black characters are nonturn-inducers (normalized turn potential < 1). Residues written in bold white characters are turn-inducers. They are highlighted according to their turn potential as follows: light green for a potential between 1.1 and 1.6 (Trp, Ser, Tyr, Thr, and Cys), medium green for a potential between 2.1 and 2.3 (His, Gln, Lys, and Glu), and dark green for a potential between 2.5 and 2.7 (Pro, Asn, Arg, and Asp). Glycine (potential = 1.9), normally abundant in turns of water-soluble and membrane proteins, is not present in these sequences. The blue bars on top of the sequences represent their secondary structure as determined for the full-length proteins in solution. The thick light-blue bar corresponds to the α helix, and the thin dark-blue bar corresponds to the connecting turn.

chimeras of Bcl-$x_L^{\alpha5}$, $Bax^{\alpha5}$, and $Bid^{\alpha6}$, with respect to the $Lep^{\Delta H1}$ fusions of their corresponding hairpins, indicates an increased insertion efficiency in favor of the hairpins. These results suggest the existence of complementarity or a synergistic insertion, between the two α-helix fragments of each hairpin. One possible source for such a complementarity might be favorable electrostatic interactions between charged residues from each of the two α helices of the hairpin, which would help in stabilizing both fragments in a TM state. Looking at the structures represented in Figure 8, one can find that charge complementarity may indeed exist. This can be more clearly envisioned in the cases of Bcl-x_L (Figure 8A) and Bax (Figure 8B), although it does not seem to be obvious in the case of Bid (Figure 8C).

An additional source of stability of the TM hairpin can be the turn between the two helices. It has been shown that charged and polar residues plus Pro and Gly display turn induction in a poly(Leu) stretch (*87*, *88*). In our case, we do not know exactly which are the amino acid residues that make the turn in the membrane-bound hairpins, although to a good approximation, we may assume that such turns are placed at positions similar to the ones found in solution. In Figure 9, we show a 15-residue extract of the interhelical region of Bcl-x_L, Bax, and Bid, where the residues are highlighted according to their turn-inducing propensities (*88*). The dominance of turn-inducing residues (normalized turn potential > 1) over noninducing ones (turn potential < 1) is clearly noticeable. Among them, more than half have a high turn potential (>2), and there are at least two residues in each region of the group with the highest turn-inducing potential (Pro, Asn, Arg, and Asp, with potential > 2.5). In essence, the highest turn promoters concentrate close to the actual turn of the hairpins found in the structures of the soluble proteins, although we can predict slight shifts toward groups of consecutive highly turn inducers. Thus, in the membrane-bound form, we can expect the turn of Bcl-$x_L^{\alpha5\alpha6}$

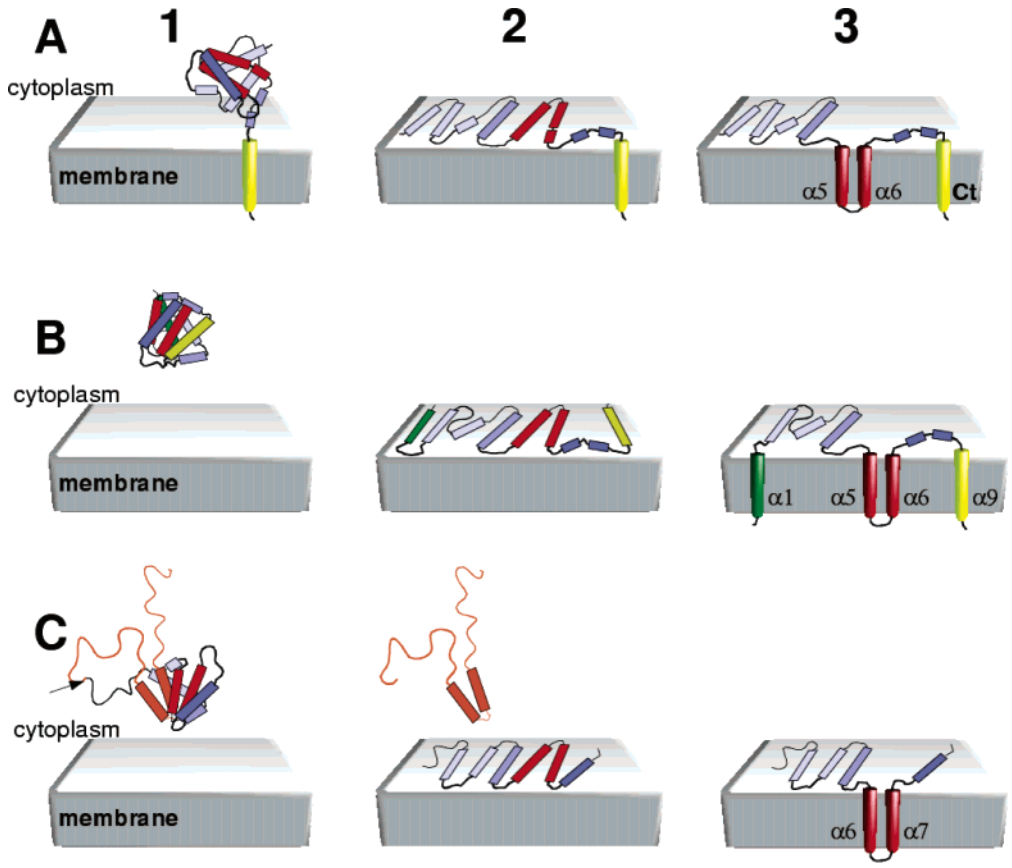

FIGURE 10: Models of membrane insertion, as simplified, two-step processes. Bcl-x_L is represented in A, with the C-terminal hydrophobic tail colored in yellow and α helices 5 and 6, in red. Bax is represented in B, with helices α1 colored in green; α5 and α6, in red; and α9, in yellow. Bid is drawn in C, where the caspase-8 cleavage site is indicated with an arrow, the N-terminal fragment is colored in orange, and helices α6 and α7 are colored in red. Column 1 corresponds to the constitutive inactive species, in the absence of apoptotic stimuli. Upon apoptotic signal triggering, the latter evolves into a membrane-inserted species, represented in column 3, passing through a hypothetical intermediate, represented in column 2. The models in 1 are based on the experimental structures of water-soluble forms of these proteins (*49*, *52*, *53*). The models in 3 are based on data from this paper, in agreement with the literature data in the case of Bcl-x_L (*65*, *66*). The models in 2 are proposed by analogy with the mechanism of insertion of the pore-forming domain of colicin E1 (*90*), taking also into account the data from refs *18*, *65*, and *91*. The transitions 1 → 2 and 2 → 3 are most likely regulated processes, with the expected interplay of other proteins not shown in the figure (see the text).

to be centered around ^{156}DKE^{158}, while in the Bax$^{\alpha5\alpha6}$ and Bid$^{\alpha6\alpha7}$ hairpins, the turn is expected to leave the Pro residue at the N terminus of the second α helix (*88*). Although in view of the short hydrophobic stretches of these TM fragments, we must consider as well the positioning of the charged residues at both ends of the α helices. In any case, it seems clear that the turns may play a significant role for the stability of the membrane-bound hairpins.

Despite the latter considerations, we notice that driving such charged fragments into a membrane environment should involve an important energetic cost that is expected to impose restrictions on the membrane-inserted state of the protein. Because these α helices are markedly amphipathic (Figure 8), it is normally assumed that charges may be shielded from the lipid bilayer through the formation of oligomeric water-filled pores (*89*). The latter structural requirement would also hold here, although we have no evidence about the formation of such structures.

Despite the fact that these data were obtained with fusion proteins, the synergistic effect found for the insertion of the α-helical hairpins support the capacity of these domains to act as TM fragments in their natural context. Moreover, it should be noticed that in the case of the Lep$^{\Delta H1}$ constructs the assayed hairpins contribute the only two TM fragments, which are present in the chimera.

Models for Membrane Insertion. On the basis of the above results and data from the literature, we propose schematic membrane-insertion models for the three proteins studied in this paper (Figure 10). The models start with constitutive *inactive* forms, found in the absence of apoptotic signals (column 1 of Figure 10) and assume the existence of intermediate species, peripherally bound to the membrane (column 2 of Figure 10), previous to the *active* membrane-inserted forms (column 3 of Figure 10). Stepwise mechanisms of insertion have been proposed before in the cases of Bax and Bcl-2 to explain different degrees of membrane/protein interaction and provide multiple levels of regulation (*18*, *29*, *65*).

Solid-state NMR data indicate that the interaction of Bcl-x_L (depleted of its C-terminal hydrophobic tail) with synthetic lipid membranes involves insertion of the α5−α6 hairpin, while the rest of the protein lays parallel to the bilayers (*66*). This *umbrella-like* model (part A3 of Figure 10) agrees with the data reported here and with cysteine modification studies of Bcl-2 (*65*). In this latter case, interaction with a BH3 domain might work as a trigger for the change of topology

from the tail-anchored form (part A1 of Figure 10). However, insertion of α5 appears to require additional proteins, because it is not observed in liposome membranes (*65*). This suggest the existence of an intermediate state, similar to the case of the pore-forming domain of colicin E1 (*90*), where it has been proposed that prior to the integral-membrane state the protein arranges in the membrane interfacial layer as an extended mobile helical array (part A2 of Figure 10).

A multistep mode of insertion may also apply to Bax. As a consequence of activation of apoptosis, cytoplasmatic Bax (part B1 of Figure 10) relocalizes at the MOM. Targeting to mitochondria is accompanied by structural changes and strong association to the lipid membrane, ending with the formation of an oligomeric pore. In this sequence of events, a change in conformation of the inactive, water-soluble form, controlled at the level of Pro168 (*29*), would act as a preliminary step that releases the C- (α9) and N-terminal (α1) hydrophobic helices (*29*). This partially open intermediate would be capable of targeting to membranes, where the structural transition proceeds to give membrane associated, though neither inserted nor oligomerized, species (part B2 of Figure 10). Evidence for a peripherally bound intermediate is provided in a recent in vitro study (*18*). In a subsequent step, probably mediated by tBid, TM insertion of fragments $Bax^{\alpha 1}$, $Bax^{\alpha 9}$, and the $Bax^{\alpha 5\alpha 6}$ hairpin may happen (part B3 of Figure 10), followed by oligomerization and pore formation.

With respect to Bid, membrane targeting must be preceded by an apoptosis activation signal, provided by the caspase-8 digestion of the inactive cytoplasmatic Bid (*23*, *24*) (part C1 of Figure 10). Interaction of the active C-terminal fragment, tBid, with synthetic lipid membranes has been recently studied by solid-state $^{1}H/^{15}N$ NMR (*91*). Surprisingly, all α helices appear to interact with the membrane in a parallel fashion, without TM helix insertion, which apparently contradicts the data presented here and previous reports claiming that tBid behaves as an integral-membrane protein (*85*). However, insertion of tBid in the membrane may require the presence of specific mitochondrial lipids, like cardiolipin (*30*), or the assistance of proteins present in the MOM. As we have discussed above, both Bcl-x_L and Bax also seem to require the assistance of specific proteins to complete their insertion. Probably, the structure observed by NMR corresponds to an intermediate membrane-bound state (part C2 of Figure 10), previous to an inserted state (part C3 of Figure 10) for which the activity of additional specific elements might be required.

CONCLUSIONS

The pBcl2s can form channels in membranes, where they also acquire their functional structures, but they are not regular membrane proteins. Despite the importance of their function, however, much is still to be known about their active, membrane-bound structures. Different domains of these proteins have been related to membrane interaction, either as C-terminal anchors, intracellular membrane targeting, or pore forming, but the evidence about the participation of these fragments as TM fragments is, in general, indirect and scarce. Clarifying the potential of segments from these proteins to insert across the membrane is of special interest, because apart from a C-terminal tail found in some of them, the rest of their sequence displays only weak hydrophobic peaks that would not qualify as TM fragments according to most prediction algorithms.

In this paper, we have analyzed in detail the sequences of three paradigmatic proteins of the pBcl2 family. Guided initially by two TM prediction methods, we selected all possible TM fragments, including some with score values below the lower cutoff. Careful analysis by glycosylation mapping allows us to conclude that, apart from the C-terminal α helices from Bcl-x_L and Bax, various weakly hydrophobic fragments from these two proteins and Bid can insert across microsomal membranes in a model chimeric system. In total, three TM fragments were found for Bcl-x_L, consisting of C-terminal helices α5 and α6; four were found in Bax, namely, α1, α5, α6, and α9; and two in the case of tBid, α6 and α7. The fragments that constitute a putative pore-forming domain in these three proteins, namely, the double-helices α5−α6 from Bcl-x_L and Bax and α6−α7 from Bid, display a singular behavior, because the second helix of these domains inserts only together with the first one, as part of a hairpin. It appears that α-helix 5 (α6 for Bid) helps in stabilizing the less hydrophobic α-helix 6 (α7 for Bid) in a TM state. Charge complementarity and stabilization of the turn by relatively abundant turn-inducing residues can help explain the observed synergism. These results show the importance of the protein context in determining the stability of the TM state of individual fragments, a factor that can be critical in the case of weakly hydrophobic segments, especially those that contain polar residues. We suggest that insertion of TM hairpins can be a useful model to investigate cooperative folding of membrane proteins.

ACKNOWLEDGMENT

We thank G. von Heijne (Stockholm University) for providing the pGEM-Lep-NST and pGEM-$Lep^{\Delta H1}$ plasmids, G. Nuñez (University of Michigan Medical School) for providing plasmids containing human Bcl-x_L and mouse Bax, and X. Wang (University of Texas Southwestern Medical Center) for a plasmid construct of human Bid.

REFERENCES

1. Gross, A., McDonnell, J. M., and Korsmeyer, S. J. (1999) BCL-2 family members and the mitochondria in apoptosis, *Genes Dev. 13*, 1899−1911.
2. Adams, J. M., and Cory, S. (1998) The Bcl-2 protein family: Arbiters of cell survival, *Science 281*, 1322−1326.
3. Monaghan, P., Robertson, D., Amos, T. A., Dyer, M. J., Mason, D. Y., and Greaves, M. F. (1992) Ultrastructural localization of Bcl-2 protein, *J. Histochem. Cytochem. 40*, 1819−1825.
4. Nguyen, M., Millar, D. G., Yong, V. W., Korsmeyer, S. J., and Shore, G. C. (1993) Targeting of Bcl-2 to the mitochondrial outer membrane by a COOH-terminal signal anchor sequence, *J. Biol. Chem. 268*, 25265−25268.
5. Janiak, F., Leber, B., and Andrews, D. W. (1994) Assembly of Bcl-2 into microsomal and outer mitochondrial membranes, *J. Biol. Chem. 269*, 9842−9849.
6. Kaufmann, T., Schlipf, S., Sanz, J., Neubert, K., Stein, R., and Borner, C. (2003) Characterization of the signal that directs Bcl-xL, but not Bcl-2, to the mitochondrial outer membrane, *J. Cell. Biol. 160*, 53−64.
7. Wolter, K. G., Hsu, Y. T., Smith, C. L., Nechushtan, A., Xi, X. G., and Youle, R. J. (1997) Movement of Bax from the cytosol to mitochondria during apoptosis, *J. Cell. Biol. 139*, 1281−1292.
8. Gross, A., Jockel, J., Wei, M. C., and Korsmeyer, S. J. (1998) Enforced dimerization of BAX results in its translocation, mitochondrial dysfunction, and apoptosis, *EMBO J. 17*, 3878−3885.

9. Desagher, S., Osen-Sand, A., Nichols, A., Eskes, R., Montessuit, S., Lauper, S., Maundrell, K., Antonsson, B., and Martinou, J. C. (1999) Bid-induced conformational change of Bax is responsible for mitochondrial cytochrome *c* release during apoptosis, *J. Cell. Biol. 144*, 891−901.
10. Oltvai, Z. N., Milliman, C. L., and Korsmeyer, S. J. (1993) Bcl-2 heterodimerizes in vivo with a conserved homolog, Bax, that accelerates programmed cell death, *Cell 74*, 609−619.
11. Sattler, M., Liang, H., Nettesheim, D., Meadows, R. P., Harlan, J. E., Eberstadt, M., Yoon, H. S., Shuker, S. B., Chang, B. S., Minn, A. J., Thompson, C. B., and Fesik, S. W. (1997) Structure of Bcl-x_L-Bak peptide complex: Recognition between regulators of apoptosis, *Science 275*, 983−986.
12. Cheng, E. H., Wei, M. C., Weiler, S., Flavell, R. A., Mak, T. W., Lindsten, T., and Korsmeyer, S. J. (2001) BCL-2, BCL-X(L) sequester BH3 domain-only molecules preventing BAX- and BAK-mediated mitochondrial apoptosis, *Mol. Cell 8*, 705−711.
13. Kelekar, A., Chang, B. S., Harlan, J. E., Fesik, S. W., and Thompson, C. B. (1997) Bad is a BH3 domain-containing protein that forms an inactivating dimer with Bcl-x_L, *Mol. Cell. Biol. 17*, 7040−7046.
14. Boise, L. H., Gonzalez-Garcia, M., Postema, C. E., Ding, L., Lindsten, T., Turka, L. A., Mao, X., Nunez, G., and Thompson, C. B. (1993) Bcl-x, a bcl-2-related gene that functions as a dominant regulator of apoptotic cell death, *Cell 74*, 597−608.
15. Hsu, Y. T., Wolter, K. G., and Youle, R. J. (1997) Cytosol-to-membrane redistribution of Bax and Bcl-X(L) during apoptosis, *Proc. Natl. Acad. Sci. U.S.A. 94*, 3668−3672.
16. Goping, I. S., Gross, A., Lavoie, J. N., Nguyen, M., Jemmerson, R., Roth, K., Korsmeyer, S. J., and Shore, G. C. (1998) Regulated targeting of BAX to mitochondria, *J. Cell. Biol. 143*, 207−215.
17. Nechushtan, A., Smith, C. L., Hsu, Y. T., and Youle, R. J. (1999) Conformation of the Bax C-terminus regulates subcellular location and cell death, *EMBO J. 18*, 2330−2341.
18. Yethon, J. A., Epand, R. F., Leber, B., Epand, R. M., and Andrews, D. W. (2003) Interaction with a membrane surface triggers a reversible conformational change in Bax normally associated with induction of apoptosis, *J. Biol. Chem. 278*, 48935−48941.
19. Eskes, R., Desagher, S., Antonsson, B., and Martinou, J. C. (2000) Bid induces the oligomerization and insertion of Bax into the outer mitochondrial membrane, *Mol. Cell. Biol. 20*, 929−935.
20. Wei, M. C., Zong, W. X., Cheng, E. H., Lindsten, T., Panoutsakopoulou, V., Ross, A. J., Roth, K. A., MacGregor, G. R., Thompson, C. B., and Korsmeyer, S. J. (2001) Proapoptotic BAX and BAK: A requisite gateway to mitochondrial dysfunction and death, *Science 292*, 727−730.
21. Roucou, X., Rostovtseva, T., Montessuit, S., Martinou, J. C., and Antonsson, B. (2002) Bid induces cytochrome *c*-impermeable Bax channels in liposomes, *Biochem. J. 363*, 547−552.
22. Wei, M. C., Lindsten, T., Mootha, V. K., Weiler, S., Gross, A., Ashiya, M., Thompson, C. B., and Korsmeyer, S. J. (2000) tBID, a membrane-targeted death ligand, oligomerizes BAK to release cytochrome *c*, *Genes Dev. 14*, 2060−2071.
23. Luo, X., Budihardjo, I., Zou, H., Slaughter, C., and Wang, X. (1998) Bid, a Bcl2 interacting protein, mediates cytochrome *c* release from mitochondria in response to activation of cell surface death receptors, *Cell 94*, 481−490.
24. Li, H., Zhu, H., Xu, C. J., and Yuan, J. (1998) Cleavage of BID by caspase 8 mediates the mitochondrial damage in the Fas pathway of apoptosis, *Cell 94*, 491−501.
25. Antonsson, B., Montessuit, S., Lauper, S., Eskes, R., and Martinou, J. C. (2000) Bax oligomerization is required for channel-forming activity in liposomes and to trigger cytochrome *c* release from mitochondria, *Biochem. J. 345*, 271−278.
26. Antonsson, B., Montessuit, S., Sanchez, B., and Martinou, J. C. (2001) Bax is present as a high molecular weight oligomer/complex in the mitochondrial membrane of apoptotic cells, *J. Biol. Chem. 276*, 11615−11623.
27. Korsmeyer, S. J., Wei, M. C., Saito, M., Weiler, S., Oh, K. J., and Schlesinger, P. H. (2000) Pro-apoptotic cascade activates BID, which oligomerizes BAK or BAX into pores that result in the release of cytochrome *c*, *Cell Death Differ. 7*, 1166−1173.
28. Cartron, P. F., Priault, M., Oliver, L., Meflah, K., Manon, S., and Vallette, F. M. (2003) The N-terminal end of Bax contains a mitochondrial-targeting signal, *J. Biol. Chem. 278*, 11633−11641.
29. Schinzel, A., Kaufmann, T., Schuler, M., Martinalbo, J., Grubb, D., and Borner, C. (2004) Conformational control of Bax localization and apoptotic activity by Pro168, *J. Cell Biol. 164*, 1021−1032.
30. Lutter, M., Fang, M., Luo, X., Nishijima, M., Xie, X., and Wang, X. (2000) Cardiolipin provides specificity for targeting of tBid to mitochondria, *Nat. Cell Biol. 2*, 754−761.
31. Kuwana, T., Mackey, M. R., Perkins, G., Ellisman, M. H., Latterich, M., Schneiter, R., Green, D. R., and Newmeyer, D. D. (2002) Bid, Bax, and lipids cooperate to form supramolecular openings in the outer mitochondrial membrane, *Cell 111*, 331−342.
32. Crompton, M. (2000) Bax, Bid, and the permeabilization of the mitochondrial outer membrane in apoptosis, *Curr. Opin. Cell. Biol. 12*, 414−419.
33. Roucou, X., Montessuit, S., Antonsson, B., and Martinou, J. C. (2002) Bax oligomerization in mitochondrial membranes requires tBid (caspase-8-cleaved Bid) and a mitochondrial protein, *Biochem. J. 368*, 915−921.
34. Minn, A. J., Velez, P., Schendel, S. L., Liang, H., Muchmore, S. W., Fesik, S. W., Fill, M., and Thompson, C. B. (1997) Bcl-x(L) forms an ion channel in synthetic lipid membranes, *Nature 385*, 353−357.
35. Schendel, S. L., Azimov, R., Pawlowski, K., Godzik, A., Kagan, B. L., and Reed, J. C. (1999) Ion channel activity of the BH3 only Bcl-2 family member, BID, *J. Biol. Chem. 274*, 21932−21936.
36. Schendel, S. L., Xie, Z., Montal, M. O., Matsuyama, S., Montal, M., and Reed, J. C. (1997) Channel formation by antiapoptotic protein Bcl-2, *Proc. Natl. Acad. Sci. U.S.A. 94*, 5113−5118.
37. Antonsson, B., Conti, F., Ciavatta, A., Montessuit, S., Lewis, S., Martinou, I., Bernasconi, L., Bernard, A., Mermod, J. J., Mazzei, G., Maundrell, K., Gambale, F., Sadoul, R., and Martinou, J. C. (1997) Inhibition of Bax channel-forming activity by Bcl-2, *Science 277*, 370−372.
38. Marzo, I., Brenner, C., Zamzami, N., Jurgensmeier, J. M., Susin, S. A., Vieira, H. L., Prevost, M. C., Xie, Z., Matsuyama, S., Reed, J. C., and Kroemer, G. (1998) Bax and adenine nucleotide translocator cooperate in the mitochondrial control of apoptosis, *Science 281*, 2027−2031.
39. Narita, M., Shimizu, S., Ito, T., Chittenden, T., Lutz, R. J., Matsuda, H., and Tsujimoto, Y. (1998) Bax interacts with the permeability transition pore to induce permeability transition and cytochrome *c* release in isolated mitochondria, *Proc. Natl. Acad. Sci. U.S.A. 95*, 14681−14686.
40. Shimizu, S., Narita, M., and Tsujimoto, Y. (1999) Bcl-2 family proteins regulate the release of apoptogenic cytochrome *c* by the mitochondrial channel VDAC, *Nature 399*, 483−487.
41. Brenner, C., Cadiou, H., Vieira, H. L., Zamzami, N., Marzo, I., Xie, Z., Leber, B., Andrews, D., Duclohier, H., Reed, J. C., and Kroemer, G. (2000) Bcl-2 and Bax regulate the channel activity of the mitochondrial adenine nucleotide translocator, *Oncogene 19*, 329−336.
42. Zong, W. X., Li, C., Hatzivassiliou, G., Lindsten, T., Yu, Q. C., Yuan, J., and Thompson, C. B. (2003) Bax and Bak can localize to the endoplasmic reticulum to initiate apoptosis, *J. Cell. Biol. 162*, 59−69.
43. Nutt, L. K., Pataer, A., Pahler, J., Fang, B., Roth, J., McConkey, D. J., and Swisher, S. G. (2002) Bax and Bak promote apoptosis by modulating endoplasmic reticular and mitochondrial Ca^{2+} stores, *J. Biol. Chem. 277*, 9219−9225.
44. Scorrano, L., Oakes, S. A., Opferman, J. T., Cheng, E. H., Sorcinelli, M. D., Pozzan, T., and Korsmeyer, S. J. (2003) BAX and BAK regulation of endoplasmic reticulum Ca^{2+}: A control point for apoptosis, *Science 300*, 135−139.
45. Shimizu, S., Konishi, A., Kodama, T., and Tsujimoto, Y. (2000) BH4 domain of antiapoptotic Bcl-2 family members closes voltage-dependent anion channel and inhibits apoptotic mitochondrial changes and cell death, *Proc. Natl. Acad. Sci. U.S.A. 97*, 3100−3105.
46. Minn, A. J., Kettlun, C. S., Liang, H., Kelekar, A., van der Heiden, M. G., Chang, B. S., Fesik, S. W., Fill, M., and Thompson, C. B. (1999) Bcl-x_L regulates apoptosis by heterodimerization-dependent and -independent mechanisms, *EMBO J. 18*, 632−643.
47. Smaili, S. S., Hsu, Y. T., Youle, R. J., and Russell, J. T. (2000) Mitochondria in Ca^{2+} signaling and apoptosis, *J. Bioenerg. Biomembr. 32*, 35−46.
48. Pinton, P., Ferrari, D., Rapizzi, E., di Virgilio, F., Pozzan, T., and Rizzuto, R. (2002) A role for calcium in Bcl-2 action? *Biochimie 84*, 195−201.
49. Muchmore, S. W., Sattler, M., Liang, H., Meadows, R. P., Harlan, J. E., Yoon, H. S., Nettesheim, D., Chang, B. S., Thompson, C. B., Wong, S. L., Ng, S. L.. and Fesik, S. W. (1996) X-ray and

NMR structure of human Bcl-x_L, an inhibitor of programmed cell death, *Nature 381*, 335−341.
50. Aritomi, M., Kunishima, N., Inohara, N., Ishibashi, Y., Ohta, S., and Morikawa, K. (1997) Crystal structure of rat Bcl-x_L. Implications for the function of the Bcl-2 protein family, *J. Biol. Chem. 272*, 27886−27892.
51. Petros, A. M., Medek, A., Nettesheim, D. G., Kim, D. H., Yoon, H. S., Swift, K., Matayoshi, E. D., Oltersdorf, T., and Fesik, S. W. (2001) Solution structure of the antiapoptotic protein bcl-2, *Proc. Natl. Acad. Sci. U.S.A. 98*, 3012−3017.
52. Suzuki, M., Youle, R. J., and Tjandra, N. (2000) Structure of Bax. Coregulation of dimer formation and intracellular localization, *Cell 103*, 645−654.
53. McDonnell, J. M., Fushman, D., Milliman, C. L., Korsmeyer, S. J., and Cowburn, D. (1999) Solution structure of the proapoptotic molecule BID: A structural basis for apoptotic agonists and antagonists, *Cell 96*, 625−634.
54. Chou, J. J., Li, H. L., Salvesen, G. S., Yuan, J. Y., and Wagner, G. (1999) Solution structure of BID, an intracellular amplifier of apoptotic signaling, *Cell 96*, 615−624.
55. Cramer, W. A., Heymann, J. B., Schendel, S. L., Deriy, B. N., Cohen, F. S., Elkins, P. A., and Stauffacher, C. V. (1995) Structure−function of the channel-forming colicins, *Annu. Rev. Biophys. Biomol. Struct. 24*, 611−641.
56. Stroud, R. M., Reiling, K., Wiener, M., and Freymann, D. (1998) Ion-channel-forming colicins, *Curr. Opin. Struct. Biol. 8*, 525−533.
57. Schlesinger, P. H., Gross, A., Yin, X. M., Yamamoto, K., Saito, M., Waksman, G., and Korsmeyer, S. J. (1997) Comparison of the ion channel characteristic of proapoptotic Bax and antiapoptotic Bcl-2, *Proc. Natl. Acad. Sci. U.S.A. 94*, 11357−11362.
58. Saito, M., Korsmeyer, S. J., and Schlesinger, P. H. (2000) Bax-dependent transport of cytochrome *c* reconstituted in pure liposomes, *Nat. Cell Biol. 2*, 553−555.
59. Pinton, P., Ferrari, D., Rapizzi, E., Virgilio, F. D., Di/Pozzan, T., and Rizzuto, R. (2001) The Ca^{2+} concentration of the endoplasmic reticulum is a key determinant of ceramide-induced apoptosis: Significance for the molecular mechanism of Bcl-2 action, *EMBO J. 20*, 2690−2701.
60. Rudner, J., Jendrossek, V., and Belka, C. (2002) New insights in the role of Bcl-2. Bcl-2 and the endoplasmic reticulum, *Apoptosis 7*, 441−447.
61. Nutt, L. K., Chandra, J., Pataer, A., Fang, B., Roth, J. A., Swisher, S. G., O'Neil, R. G., and McConkey, D. J. (2002) Bax-mediated Ca^{2+} mobilization promotes cytochrome *c* release during apoptosis, *J. Biol. Chem. 277*, 20301−20308.
62. Matsuyama, S., Schendel, S. L., Xie, Z., and Reed, J. C. (1998) Cytoprotection by Bcl-2 requires the pore-forming α5 and α6 helices, *J. Biol. Chem. 273*, 30995−31001.
63. Nouraini, S., Six, E., Matsuyama, S., Krajewski, S., and Reed, J. C. (2000) The putative pore-forming domain of Bax regulates mitochondrial localization and interaction with Bcl-X(L), *Mol. Cell. Biol. 20*, 1604−1615.
64. Heimlich, G., McKinnon, A. D., Bernardo, K., Brdiczka, D., Reed, J. C., Kain, R., Kronke, M., and Jurgensmeier, J. M. (2004) Bax-induced cytochrome *c* release from mitochondria depends on α-helices-5 and -6, *Biochem. J. 378*, 247−255.
65. Kim, P. K., Annis, M. G., Dlugosz, P. J., Leber, B., and Andrews, D. W. (2004) During apoptosis bcl-2 changes membrane topology at both the endoplasmic reticulum and mitochondria, *Mol. Cell 14*, 523−529.
66. Franzin, C. M., Choi, J., Zhai, D., Reed, J. C., and Marassi, F. M. (2004) Structural studies of apoptosis and ion transport regulatory proteins in membranes, *Magn. Reson. Chem. 42*, 172−179.
67. Claros, M. G., and von Heijne, G. (1994) TopPred II: An improved software for membrane protein structure predictions, *Comput. Appl. Biosci. 10*, 685−686.
68. Cserzo, M., Wallin, E., Simon, I., von Heijne, G., and Elofsson, A. (1997) Prediction of transmembrane α-helices in prokaryotic membrane proteins: The dense alignment surface method, *Protein Eng. 10*, 673−676.
69. Nielsen, H., Engelbrecht, J., Brunak, S., and von Heijne, G. (1997) Identification of prokaryotic and eukaryotic signal peptides and prediction of their cleavage sites, *Protein Eng. 10*, 1−6.
70. Nilsson, I., Whitley, P., and von Heijne, G. (1994) The COOH-terminal ends of internal signal and signal-anchor sequences are positioned differently in the ER translocase, *J. Cell. Biol. 126*, 1127−1132.
71. Nilsson, I., and von Heijne, G. (1998) Breaking the camel's back: Proline-induced turns in a model transmembrane helix, *J. Mol. Biol. 284*, 1185−1189.
72. Nilsson, I. M., and von Heijne, G. (1993) Determination of the distance between the oligosaccharyltransferase active site and the endoplasmic reticulum membrane, *J. Biol. Chem. 268*, 5798−5801.
73. Vilar, M., Sauri, A., Monne, M., Marcos, J. F., von Heijne, G., Perez-Paya, E., and Mingarro, I. (2002) Insertion and topology of a plant viral movement protein in the endoplasmic reticulum membrane, *J. Biol. Chem. 277*, 23447−23452.
74. Nilsson, I., Johnson, A. E., and von Heijne, G. (2002) Cleavage of a tail-anchored protein by signal peptidase, *FEBS Lett. 516*, 106−108.
75. Whitley, P., Grahn, E., Kutay, U., Rapoport, T. A., and von Heijne, G. (1996) A 12-residue-long polyleucine tail is sufficient to anchor synaptobrevin to the endoplasmic reticulum membrane, *J. Biol. Chem. 271*, 7583−7586.
76. Schaad, M. C., Jensen, P. E., and Carrington, J. C. (1997) Formation of plant RNA virus replication complexes on membranes: Role of an endoplasmic reticulum-targeted viral protein, *EMBO J. 16*, 4049−4059.
77. Bordier, C. (1981) Phase separation of integral membrane proteins in Triton X-114 solution, *J. Biol. Chem. 256*, 1604−1607.
78. von Heijne, G. (1992) Membrane protein structure prediction. Hydrophobicity analysis and the positive-inside rule, *J. Mol. Biol. 225*, 487−494.
79. Kyte, J., and Doolittle, R. F. (1982) A simple method for displaying the hydropathic character of a protein, *J. Mol. Biol. 157*, 105−132.
80. van Geest, M., and Lolkema, J. S. (2000) Membrane topology and insertion of membrane proteins: Search for topogenic signals, *Microbiol. Mol. Biol. Rev. 64*, 13−33.
81. von Heijne, G. (1989) Control of topology and mode of assembly of a polytopic membrane protein by positively charged residues, *Nature 341*, 456−458.
82. van Geest, M., Nilsson, I., von Heijne, G., and Lolkema, J. S. (1999) Insertion of a bacterial secondary transport protein in the endoplasmic reticulum membrane, *J. Biol. Chem. 274*, 2816−2823.
83. Borgese, N., Colombo, S. and Pedrazzini, E. (2003) The tale of tail-anchored proteins: Coming from the cytosol and looking for a membrane, *J. Cell Biol. 161*, 1013−1019.
84. Peremyslov, V. V., Pan, Y. W., and Dolja, V. V. (2004) Movement protein of a closterovirus is a type III integral transmembrane protein localized to the endoplasmic reticulum, *J. Viriol. 78*, 3704−3709.
85. Gross, A., Yin, X. M., Wang, K., Wei, M. C., Jockel, J., Milliman, C., Erdjument-Bromage, H., Tempst, P., and Korsmeyer, S. J. (1999) Caspase cleaved BID targets mitochondria and is required for cytochrome *c* release, while BCL-x_L prevents this release but not tumor necrosis factor-R1/Fas death, *J. Biol. Chem. 274*, 1156−1163.
86. Losonczi, J. A., Olejniczak, E. T., Betz, S. F., Harlan, J. E., Mack, J., and Fesik, S. W. (2000) NMR studies of the anti-apoptotic protein Bcl-x_L in micelles, *Biochemistry 39*, 11024−11033.
87. Monne, M., Hermansson, M., and von Heijne, G. (1999) A turn propensity scale for transmembrane helices, *J. Mol. Biol.* 288, 141−145.
88. Monne, M., Nilsson, I., Elofsson, A., and von Heijne, G. (1999) Turns in transmembrane helices: Determination of the minimal length of a helical hairpin and derivation of a fine-grained turn propensity scale, *J. Mol. Biol. 293*, 807−814.
89. Schendel, S. L., Montal, M., and Reed, J. C. (1998) Bcl-2 family proteins as ion-channels, *Cell Death Differ. 5*, 372−380.
90. Zakharov, S. D., and Cramer, W. A. (2002) Insertion intermediates of pore-forming colicins in membrane two-dimensional space, *Biochimie 84*, 465−475.
91. Gong, X. M., Choi, J., Franzin, C. M., Zhai, D., Reed, J. C., and Marassi, F. M. (2004) Conformation of membrane-associated pro-apoptotic tBid, *J. Biol. Chem. 279*, 28954−28960.

BI036044C